Volatile fatty acid adsorption on anion exchange resins: kinetics and selective recovery of acetic acid

Tejaswini Eregowda[1,2,*], Eldon R. Rene[1], Jukka Rintala[2], Piet N. L. Lens[1,2]

[1] UNESCO-IHE, Institute for Water Education, P. O. Box 3015, 2601 DA Delft, The Netherlands

[2] Department of Chemistry and Bioengineering, Tampere University of Technology, P. O. Box 541, Tampere, Finland

Declaration of interest: *none*

[**]**Corresponding author**

Eldon R. Rene

UNESCO-IHE, Institute for Water Education

P. O. Box. 3015, 2601DA Delft, The Netherlands

E-mail: e.raj@un-ihe.org

Tel: +31-152151840

Abstract

The removal of volatile fatty acids were examined through adsorption on anion exchange resins in batch systems. During the initial screening step, granular activated carbon and 11 anion exchange resins were tested and the resins Amberlite IRA-67 and Dowex optipore L-493 were chosen for further investigation. The adsorption kinetics and diffusion mechanism and adsorption isotherms of the two resins for VFA were evaluated. Based on the selective adsorption capacity of the resins, a sequential batch process was tested to achieve separation of acetic acid from the VFA mixture and selective recoveries >85% acetic acid and ~75% propionic acid was achieved.

Keywords: Volatile fatty acids; selective recovery; anion-exchange resins; Brunauer-Emmett-Teller model;

1. Introduction

Volatile fatty acids (VFA) are used in a wide range of industries such as chemicals, polymers, food and agriculture. Most of these VFA are currently produced by the photo-catalysis of refined heavy oil and natural gas [1]. In recent years, the recovery of VFA from the biological treatment of wastewater, sewage sludge, food and fermentation waste and lignocellulosic waste biomass through dark fermentation and anaerobic digestion processes have gained a lot of interest due to the economic value of the recovered VFA [2–7]. Furthermore, in anaerobic digesters and fermenters, the removal of excess VFA is beneficial for improving the process stability and performance because VFA are primary inhibitory intermediates in the process [3].

Several studies have reported that the recovery of individual VFA from bioreactors is more challenging than its production due to the similarities in their physico-chemical properties [8–12]. Among the conventional physico-chemical recovery processes like electro-dialysis [3,13], fractional distillation, crystallization, precipitation, liquid-liquid extraction [12], adsorption on ion exchange resins[6,11,14–16] is a potential approach for the selective recovery of the desired VFA [17]. Although adsorption is generally based on the physical interaction between the adsorbent and the adsorbate, i.e. the VFA molecules, ion exchange is additionally based on chemisorption, wherein the formation of the ionic bonds between ionized carboxylic acid molecules and the cationic functional group of the anion exchange resin drives the process [17]. The performance of the ion exchange process for VFA recovery depends on the type of resin used, adsorption capacity of the resin, pH [14], temperature [18], type of desorption and the desorbing chemical used [19], presence of other competing anions [20] and the adsorption/contact time [21]. In order to ameliorate the understanding of VFA recovery through adsorption, studies pertaining to several aspects (Table 1) have been reported in the literature.

However, there still exists a knowledge gap regarding the kinetics and mechanism of VFA adsorption on ion exchange resins. Furthermore, the separation of individual VFA using a combination of resins has not been reported in the literature. Therefore, batch adsorption experiments using single- and multi-component VFA were carried out to determine the kinetics and mechanism of VFA adsorption by the resins. Accordingly, the objectives of this study were: (i) to screen the anion exchange resins that are suitable for VFA adsorption, (ii) to determine the adsorption kinetics, mechanism and isotherm for the selected resins, and (iii) to examine the selective adsorption of individual VFA from a mixture of acetic (H-ac), propionic (H-pr), isobutyric (H-ib), butyric (H-bu), isovaleric (H-iv), valeric (H-va) acid using sequential batch adsorption and a combination of resins.

2. Material and methods

2.1 Adsorption experiments

The properties (given by the manufacturers) of the 11 anion exchange resins and granular activated carbon (GAC) that were screened for the adsorption of VFA (H-ac, H-pr, H-ib, H-bu, H-iv and H-va) are listed in Table 2. Batch adsorption experiments were carried out at the corresponding pK_a value of the aqueous VFA mixture, in 110 mL gastight serum bottles with a liquid volume of 50 mL without any resin pre-treatment. Experiments were performed in either duplicates or triplicates, at room temperature (22 ± 2 ^oC) on a rotary shaker at 200 rpm. The VFA concentration was monitored by collecting the liquid-phase samples, at regular time intervals as required for the individual adsorption tests. The collected samples were stored at 4 ^oC prior to analysis. The VFA concentrations were analysed using either a Shimadzu GC-2010 or Varian GC-430 gas chromatograph, both fitted with a flame ionization detector (FID) and a ZB-WAX plus (30 m × 0.25 mm) column or CP WAX-58 CB (30 m × 0.25 mm) column. Helium was used as the carrier gas. The oven temperature was maintained at 40 ^oC for 2 min,

thereafter a ramp of 20 ^{o}C/min to reach 160 ^{o}C and another ramp of 40 ^{o}C/min to 220 ^{o}C and then maintained at 220 ^{o}C for 2 min.

2.2 Adsorption kinetics

The physical properties of the selected resins Amberlite IRA-67 (Amberlite) and Dowex Optipore L-493 (Dowex) are described in Table 3. The adsorption kinetics of Amberlite and Dower was determined for a mixture containing 1 g/L each VFA (total: 6 g/L), at resin concentrations of 25, 50 and 75 g/L. The liquid samples were collected at intervals of 0, 2, 4, 6, 8 and 24 h from the batch bottles that were tested for 1 d and at intervals of 5, 10, 15, 20, 40, 60, 80, 100 and 120 min from the batch bottles that were tested for 2 h. The percentage adsorption and the equilibrium adsorption capacity were determined using Eq.1 and Eq. 2:

$$\text{Percentage adsorption} = \frac{(C_0 - C_e)\times 100}{C_0} \quad \text{(Eq. 1)}$$

$$\text{Equilibrium adsorption capacity (mg/g)}, q_e = \frac{(C_0 - C_e)\times V}{m} \quad \text{(Eq. 2)}$$

To describe the kinetics of VFA adsorption, the pseudo-first-order, the pseudo-second-order and the Elovich's models were used. The differential and linear equations of the models are shown in Eq. 3–5; Table 4, where, K_1 is the pseudo-first-order rate constant (min^{-1}), q_e is the amount of adsorbate in the adsorbent under equilibrium conditions (mg/g), t is the time of incubation (min), q_t is the adsorption at any given point of time (mg/g), K_2 is the pseudo-second-order rate constant (mg/g.min), h_0 is the initial adsorption rate (min^{-1}), β is the desorption constant (g/mg) and α is the initial adsorption rate (mg/g.min). Intraparticle diffusion model (Eq. 6; Table 4) was used to examine the diffusion mechanism of the VFA molecules on the resin surface where, K_{id} (mg/g.min$^{-0.5}$) is intraparticle diffusion rate constant and C_{id} (mg/g) gives an approximation of the boundary layer thickness.

2.3 Resin regeneration

The regeneration of the resin and the recovery of VFA through desorption was studied at different initial concentrations of NaOH (45, 60, 70, 80, 100 mM). After adsorption, the resins were subjected to treatment with NaOH for 2 h and samples were collected once every 20 min for 2 h.

2.4 Adsorption isotherm

The VFA adsorption isotherm for the single-component and multi-component systems were evaluated using the equilibrium adsorption capacity values (Eq. 2) for Amberlite and Dowex (50 g/L), at different initial concentrations of VFA. The VFA adsorption process was elucidated using the Freundlich's single- and multi-component models and the Brunauer-Emmet-Teller (BET) model (Eq. 7–9; Table 4). In these models, E is the VFA recovery efficiency (%, expressed for the individual VFA), C_0 is the initial concentration of each VFA (mg/L), C_e is the equilibrium concentration of each VFA in the solution (mg/L), V is the volume of the solution (L), m is the mass of the adsorbent (g), q_e is the amount of adsorbate in the adsorbent under equilibrium conditions (mg/g), Q_0 is the maximum monolayer coverage capacities (mg/g), b is the Langmuir's isotherm constant (L/mg), K_F is the Freundlich's isotherm constant (mg/g) where $(L/g)^n$ is related to the adsorption capacity, n is the adsorption intensity, $C_s = 1/K_L$ (L/mg), q_s is the theoretical isotherm saturation capacity (mg/g) and K_s is the BET equilibrium constant of adsorption for the first layer relating to the energy of surface interaction (L/mg).

2.5 Selective adsorption of VFA

Based on the q_e values of Dowex and Amberlite for the individual VFA, a sequential batch adsorption experiment was designed to selectively adsorb the individual VFA. The VFA mixture containing 1g/L of individual VFA (total: 6 g/L) was first equilibrated with 25 g/L of

Dowex for 30 min. Thereafter, the liquid-phase was transferred to a 110 mL serum bottle containing 25 g/L of Amberlite and equilibrated for 30 min. For the desorption step, the resins were treated with 100 mM NaOH for 30 min. The liquid samples were analysed for initial and final VFA concentrations after both the adsorption and desorption step.

3 Results and discussion

3.1 Screening of resins

In this study, 11 different anion-exchange resins and granular activated carbon (GAC) (Table 2) that were previously examined for the adsorption of anions such as sulfate, selenate (SeO_4^{2-}) [23] and lactate [21] were examined for VFA adsorption. The percentage adsorption of resins namely, Dowex 1X8-100 (Cl), Dowex 21K XLT, Reillex 425, Dowex marathon A2 (Cl), Dowex ion exchange resin, Amberlite IRA-400 (Cl) and Amberlite IRA-900 (Cl) was < 30%, whereas the resins Amberlite IRA-67 free base, Amberlite IRA-96 free base, Dowex Optipore L-493 and granular activated carbon (GAC) (Table1) showed adsorption efficiencies > 50% (Figure 1). GAC showed 50% adsorption for H-ac and > 98% for H-va and the percentage adsorption increased with the aliphatic chain length (ACL) of the VFA. Amberlite IRA-67 (resin no. 7) showed an adsorption > 95% for all VFA, while Amberlite IRA-96 showed adsorption in the range of 75-90%. Both Amberlite IRA-67 and IRA-96 are weakly basic (type 2) resins with polyamine functional group (Table 2).

Among the wide range of adsorbents recommended in the literature for the VFA adsorption [9,11,14,19,20], type 2 (weakly basic) anion exchange resins are usually preferred because the tertiary amine functional group can adsorb carboxylic acids as charge-neutral units to maintain the charge neutrality [20]. Dowex showed < 20% adsorption for H-ac and up to 90% adsorption for H-va, and the adsorption efficiency increased with the ACL. Based on the resin screening experiment, Amberlite showed the highest adsorption for all the VFA and the VFA adsorption

by Dowex was based on the ACL. Hence, Amberlite and Dowex were selected for further experiments on the adsorption of single- and multi-component VFA.

3.2 Effect of resin concentration

In order to study the effect of resin concentration and contact time on VFA adsorption, an aqueous mixture containing 1 g/L of individual VFA (total: 6 g/L) was incubated separately with Amberlite and Dowex for 24 h. Figure 2(a1–a3) shows the percentage adsorption of Amberlite and it is evident that the adsorption of all the 6 VFA in the mixture occurred to the same extent. About 70–80% adsorption of all the VFA occurred for Amberlite at a resin concentration of 25 g/L and at a resin concentration of 50 g/L the adsorption was > 95%.

In the case of Dowex (Figure 2b1–b3), the percentage adsorption increased with an increase in the resin concentration and the ACL. At a resin concentration of 75 g/L, the percentage adsorption for H-va and H-iv was > 90%, ~ 75% for H-bu and H-ib, ~ 40% for H-pr and < 10% for H-ac, respectively. However, it is noteworthy to mention that for both Amberlite and Dowex the percentage adsorption did not vary much (< 3%) between the straight chain VFA compounds and their isomeric counterparts. Since the effect of the resin concentration on the percentage adsorption also depends on the initial VFA concentration in the liquid-phase, isotherm studies were carried out to determine the adsorption capacities of Amberlite and Dowex.

3.3 Effect of contact time

For the batches incubated for 24 h, the adsorption equilibrium was achieved and the adsorption was nearly complete within 2 h of incubation at all the three resin concentrations (Figure 2a4 and 2b4). Incubation period of 2 h [14] and 1 h [20] is usually recommended to achieve a solid-liquid equilibrium for VFA adsorption. To examine the actual time required to attain equilibrium, batch studies with 50 g/L of Amberlite and 75 g/L of Dowex was performed with

an incubation time of 2 h and samples were collected at intervals of 5, 10, 15, 20, 40, 60, 80, 100 and 120 min (Figure 2.a4 and 2.b4). The percentage adsorption increased exponentially with incubation time for both Amberlite and Dowex, and ~ 50% of the total VFA adsorption occurred within 5 min of incubation and the equilibrium adsorption was achieved within 20 min of incubation. Based on these results, an equilibrium time of 30 min was selected for the subsequent experiments.

3.4 Kinetics of VFA adsorption

In order to interpret the nature of adsorption kinetics and its mechanism, the experimental data was fitted to the pseudo-first-order (Eq. 3), pseudo-second-order (Eq. 5), Elovich (Eq. 4) and intraparticle diffusion models. The model fitted profiles for Amberlite and Dowex are shown in Figures 3(a1–a3) and 3(b1–b3), respectively. The results showed that the pseudo-second-order kinetics described the VFA adsorption data best with the highest R^2 values (Table 5), implying that the adsorption of VFA by the resins occurred through chemisorption and the sharing or exchange of electrons between the adsorbate and the adsorbent was the rate-limiting step during the adsorption process [24]. From the linearized plot of t/q_t vs. t (Figure. 3 a2 and 3b2), the pseudo-second-order constants namely q_e, h_o and K_2 were determined (Table 5). For Amberlite, the q_e, i.e. the equilibrium adsorption capacity, values of all the VFA were similar and in the range of 19.32–20.7 mg/g, whereas for Dowex, the q_e values varied between 1.31 (H-ac) and 19.98 (H-va) mg/g. The K_2 values (pseudo-second-order constant) for Amberlite followed the order: H-va and H-iv > H-bu and H-ib > H-pr > H-ac. Concerning Dowex, the K_2 value for H-ac was the highest (0.258 g/mg.min) and least for H-va (0.015 g/mg.min). Comparing the h_0 and K_2 of H-ac and H-va, the adsorption rate of H-ac (H-ac showed a much higher K_2 value) was not proportional to the number of unoccupied sites, which is not consistent with the observed low q_e value. Furthermore, high h_o for H-ac suggest a rather fast adsorption process, which should correspond to a high q_e value compared to other VFA. Nevertheless, the

observed low q_e value for H-ac when compared to other VFA implies that the exchange of electrons at the surface of the resin was not the rate limiting step for the adsorption of H-ac, rather the mechanism through which the molecules are transported to the charged surface of the resin.

3.5 Diffusion mechanism for VFA adsorption

Synthetic ion-exchange resins are usually macroporous polymeric material with a large surface area (e.g. surface area of Dowex: ~ 1100 m^2/g). The functional groups of these resins are located in the pores as well as on the surface. In completely stirred batch adsorption experiments, the mass transfer characteristics can be related to the diffusion coefficient by fitting the experimental adsorption rate data to diffusion based models. In such systems, the intraparticle diffusion model can help in understanding the diffusion mechanism of the adsorbate from the bulk liquid-phase to the resin surface [24,25]. From an engineering viewpoint, the sorption process is controlled by diffusion if its rate depends on the rate at which the adsorbate diffuse towards the charged surface site on the resin.

The linear form of the intraparticle diffusion model can be visualised by plotting q_e vs. $t^{0.5}$. If the plot is a straight line, the adsorption is controlled solely by intraparticle diffusion. On the other hand, if the data exhibits multi-linear plots, two or more steps could influence the adsorption process [24,26]. From Figures 4a and 4b, it is evident that the data points correspond to two straight lines, with the first line representing macropore diffusion and the second line representing micropore diffusion [23,24]. The intraparticle diffusion rate constant K_{id} ($mg/g.min^{-0.5}$) and C_{id} (mg/g), which gives an approximation of the boundary layer thickness, were calculated using the intra-particle diffusion model (Eq. 6). Apparently, both K_{id} and C_{id} increased with the ACL for both Amberlite and Dowex (Table 6). At the tested initial VFA concentrations, the magnitude of the difference in K_{id} and C_{id} values between the shortest (H-

ac) and the longest (H-va) VFA were much higher for Dowex, while the values were comparable for Amberlite.

3.6 Desorption and VFA recovery

For the successful application of VFA adsorption at an industrial scale, recovery of the adsorbed VFA and regeneration of the resins through desorption is crucial. In this study, desorption of ~ 1000 mg/L of individual VFA using different molar strengths of NaOH (45, 60, 70, 75, 80, 100 mM) was tested. Figure 5a–5f shows the profiles of percentage desorption of VFA from Amberlite. The desorption efficiency increased with an increase in the molar strength of NaOH, due to the increased availability of OH^- ions to displace the VFA molecules from the active site. The NaOH strength was selected based on the cumulative molar strength of the VFA mixture (~ 73 mM). Since a desorption efficiency > 98% for all the VFA was achieved using 100 mM of NaOH, it is evident that the VFA desorption through ionic displacement was driven by the concentration gradient of the adsorbing ions. Desorption was almost instantaneous with most of it occurring within the first 5 min of incubation and desorption was almost complete within 15–20 min of incubation. Based on these results, an incubation time of 30 min was selected for future desorption experiments.

The desorption techniques typically reported in the literature involves washing with solvents, e.g. water [27], methanol [28], ethanol and propanol [18], mixture of ethanol and NaOH [14], acidic or alkali solution [27]. For the recovery of high purity compounds, the desorbate should be subjected to a post-treatment step (e.g. distillation for organic acids). Pressure or temperature swing desorption along with nitrogen stripping can also be used for the recovery of VFA from the resins [18]. For future studies, additional experiments should be conducted to examine the effect of multiple adsorption-desorption cycles on the VFA recovery and the resin

stability, and the application of desorption models to elucidate the kinetics and mechanism of the desorption process.

3.7 Adsorption isotherm

3.7.1 Langmuir's isotherm for single- and multi-component system

The equilibrium VFA concentration and the respective adsorption capacity values (q_e) at initial concentrations ranging between 0.1 and 10 g/L in single-component batch systems were fitted to the Langmuir's and Freundlich's single-component isotherms. The primary assumptions for the Langmuir's adsorption isotherm model are: (i) the adsorption occurs as a monolayer, (ii) the adsorption sites are finite, localised, identical and equivalent, and (iii) there is no lateral interaction or steric hindrance between the adsorbed molecules, nor between the adjacent sites [27,29]. The Freundlich's isotherm describes the non-ideal, reversible adsorption, and it could be applied for multi-layer adsorption over heterogeneous surfaces, wherein the amount adsorbed is the sum of adsorption that occurs at all the sites. The stronger sites are occupied first until the adsorption energy is exponentially decreased, and thereafter adsorption continues at a rather slower rate at the weaker sites [25].

The adsorption data of VFA on Dowex showed a good fit for both Freundlich and Langmuir models, whereas the adsorption data on Amberlite fitted the Freundlich model with a low R^2 value (< 85%). This observation could be attributed to the fact that VFA adsorption occurred in multi-layers, especially on Amberlite and a single layer model such as Freundlich was not able to explain the higher adsorption capacity (e.g. 169.4 and 124.1 mg/g for H-Ac with Amberlite and Dowex, respectively) than the Freundlich model prediction (e.g. 75 and 25.2 mg/g for H-Ac with Amberlite and Dowex, respectively). To compare the adsorption between Amberlite and Dowex in single- and multi-component systems, the Langmuir's isotherm model was chosen for further investigation and the profiles (data not shown) of the Langmuir's

isotherm for Dowex and Amberlite were obtained using the linear form of Eq. 7; Table 4. The model parameters namely the maximum adsorption capacity, q_e (mg/g) and b (L/mg), which represents a criteria of the adsorbent-adsorbate affinity for single-component systems were determined (Table 7).

In the single-component system, the q_m for both Amberlite and Dowex increased with the ACL of the VFA with a value of 246 and 218 mg/g for H-ac and 380 and 263 mg/g for H-va, respectively. The b values for Amberlite were in a narrow range of 6.24-7.52 × 10^{-3} L/mg, while for Dowex, the b values were in the range of 0.4 (H-ac) – 2.76 (H-va) × 10^{-3} L/mg. These results were in accordance with Traube's rule which relates the adsorption process to the surface tension. Accordingly, in homologous series, VFA cause a decrease in the surface tension to a larger degree as the length of the carbon chain increases. Besides, organic acids tend to adsorb with the carbon chain parallel to the surface of the adsorbent and each -CH_2- group contributes the same adsorption energy to the molecule [30]. Although the Traube's rule is more relevant to physical adsorption on adsorbents such as activated carbon, for the chemisorption of carboxylic acids on ion exchange resins, the additional increase in the adsorption energy with increasing carbon chain length increases the adsorption capacity of the resins [18,31].

Based on the q_m and b values obtained from the single-component system, the q_e values for the multi-component system were estimated using an extended, predictive Langmuir model (Eq. 7; Table 4). This model assumes a homogeneous surface with respect to the energy of adsorption, absence of interaction between the adsorbed species and that all the active sites are equally available for the adsorbate [17,32]. In case of Amberlite, the estimated q_m value was in the order of H-pr > H-ac > H-bu > H-va, whereas it increased with ACL for Dowex. However, neither the magnitude nor the trend of the estimated q_m and b values corresponded to the q_m and b values calculated from the experimental data (Table 7).

Furthermore, in the multi-component batch systems for Amberlite, the q_m values for all VFA varied in a narrow range (169.4 and 195.3 mg/g), compared to the single-component system (246–360 mg/g). The b values were in the range of 3.7–9.38 × 10^{-3} L/mg for Amberlite and 0.99–3.19 × 10^{-3} L/mg for Dowex, wherein H-va and H-ac had the least and the highest value, respectively. The Langmuir constants (q_m and b) were ~ 2 to 8 times higher than the estimated values indicating that the adsorption occurred in multi-layers. A comparison of the q_e for individual VFAs in single-component system, the estimated q_e for the multi-component and the actual q_e values for the multi-component system are shown in Figures 6a and 6b. Based on the fact that the q_m value was ~ 2–8 times higher than the estimated value and a lower R^2 value for Dowex, a multi-layer adsorption model was considered to describe the adsorption process.

3.7.2 BET isotherm

The BET model (Eq. 9; Table 4) was applied to the multi-component batch adsorption system data using the experimentally determined q_e and c_e values. The BET model parameters are shown in Table 7, while the plots are shown in Figure 7a and 7b. By comparing the R^2 values for the Langmuir and the BET model, it is evident that the BET model was more suitable to describe the adsorption process in batch system. The BET constants were calculated based on the method proposed by Ebadi et al. [33]. In the BET equation for gas-phase adsorption, the equilibrium constant of adsorption for the outer layer (K_L) was fixed by expressing the adsorbate concentration in the form of a relative concentration, i.e. by equating $1/K_L$ to the saturation pressure, P_S. By doing so, the number of parameters was reduced to two, i.e. q_m and K_S, and the equation was linearized. In the case of liquid-phase adsorption, it was reported that the adsorption capacity (q) does not tend towards infinity when the adsorbent is saturated [33]. Besides, adsorption will also not occur at the saturation concentration (C_s) if the surface of the adsorbent has no affinity towards the adsorbate. On the contrary, if the affinity is very high, the q values could be high despite the low adsorbent dose [33]. Thus, in the present study, BET

isotherm equation (Eq. 9), C_s does not represent the actual saturation concentration, but it is an adjustable parameter which is the inverse of K_L (equilibrium or affinity constant for upper layers, L/mg). The equilibrium constant of adsorption for the first layer K_S (L/mg) is given by $K_S = C_{BET}/C_S$.

The maximum adsorption capacities for the VFA calculated using the BET model (q_s for H-ac = 115.3 mg/g) was lower than the value calculated using the Langmuir model (q_m for H-ac = 169.4 mg/g). This observation could be verified by considering the physical significance of K_S and K_L. The constant b in the Langmuir isotherm, which establishes the affinity between the absorbent and the adsorbate molecules singularly represents the affinity of interaction because the Langmuir's model is intended to represent a monolayer adsorption. The layer of adsorbent molecules around the adsorbate is taken as a single uniform layer, leading to an overestimation of b compared to the BET model. The latter model assumes that for each adsorption site, an arbitrary number of molecules may be accommodated, and hence, adsorption is a multilayer process and the layers need not necessarily be uniform. Comparing the K_S and K_L (equilibrium constant for the first layer and the outer layers, respectively), it is evident that the K_L is ~ 100 times less than the K_S. This implies that the affinity greatly reduced in the outer layers, leading to lower maximum adsorption capacity values. In the case of Amberlite, the q_m values for different VFA were nearly similar and in the range of 104.1–111.3 mg/g, whereas for Dowex, the q_m increased with the ACL, e.g. 76 g/g for H-ac and 122.3 g/g for H-va. A similar trend was observed for the Ks and K_L values, where the values were within a similar range for Amberlite (except for H-ac), where as they increased with the increasing ACL for Dowex.

3.8 Sequential batch adsorption for separation of individual VFA

In industrial situations, the separation of individual VFA from each other and/or from other organic acids present in the fermentation broth still remains a major challenge [7]. Based on

the q_m values for VFA adsorption on Amberlite and Dowex, a sequential adsorption process was designed. Figure 8 shows the percentage adsorption and desorption on Dowex and Amberlite, respectively, for a mixture containing 1000 mg/L of each VFA in a sequential batch adsorption process. It can be clearly seen that ~ 80% H-va and H-iv were recovered from Dowex, while > 85% H-ac and ~ 75% of H-pr was recovered from Amberlite. In the case of H-bu and H-ib, 55–60% was adsorbed by Dowex and the remaining was recovered by adsorption onto Amberlite. The solid brown and yellow colouration seen in Figure 8 represents the fraction that was lost during the desorption step.

The selective separation of H-ac from the VFA mixture was driven by the differential affinity of individual VFA, especially H-ac towards Dowex. As demonstrated, under the tested conditions, Amberlite could almost completely adsorb all the tested VFA and through a combination of resins (Dowex in this case), different adsorption capacities for each VFA as compared to the q_e for individual resin were achieved. The VFA fraction that was not adsorbed by Dowex adsorbed onto Amberlite and thus, nearly complete recovery of the VFA mixture was possible. Figure 2 (b1-b3) shows a clear trend of an increase in percentage adsorption of H-ac and H-pr with an increase in the resin increasing concentration for Dowex under equilibrium conditions. For scale-up purposes, the VFA to resin ratio could also be considered in order to achieve selective adsorption of the VFA. Based on the results obtained from this batch study, the sequential adsorption process could be extended to continuous column studies along with the optimization of the reactors hydrodynamic and operational parameters. By using a combination of resins, the sequential adsorption process could be extended for the adsorption of ionic compounds like sulfate, selenate and other organic acids. The challenge of interference of similarly charged ions (for example, sulfate and chloride ions interfering in the adsorption of VFA) could be overcome by selective separation through sequential batch adsorption using two or more resins, provided with appropriate choice of resin. As reported in the literature, the

Type 2 weak anion exchange resins, e.g. Amberlite IRA-67, are good candidates for the adsorption of anions such as selenate, sulphate [23], lactic acid [19,34], H-ac and H-bu [19]. Polystyrene- divinylbenzene resins, e.g. Dowex Optiopore L-493, which has high preference for H-ac as demonstrated in this study, and Lewatit VP OC 1064 MD PH, which is selective to adsorb H-Bu [20], can also be considered for the selective separation of individual VFA or other anions.

4 Conclusions

This study explored the adsorption of a mixture of VFA containing H-ac, H-pr, H-ib, H-bu, H-iv and H-va on to anion exchange resins. Anion exchange resins suited for VFA adsorption were screened and the kinetics and the adsorption capacity of two selected resins (namely Amberlite IRA and Dowex Optipore L-493) were compared. Based on the adsorption capacities of the resins for different VFA, selective separation of individual VFA was possible using a sequential batch adsorption step involving two resins. From a practical viewpoint, for *in-situ* product recovery, the sequential batch adsorption process could also be further extended for the recovery and purification of prospective second-generation biofuels.

Acknowledgements

The authors thank asst. prof. Marika E. Kokko (TUT, Finland) for her suggestions and comments during the planning of the adsorption experiments. This work was supported by the Marie Skłodowska-Curie European Joint Doctorate (EJD) in Advanced Biological Waste-to-Energy Technologies (ABWET) funded by Horizon 2020 under the grant agreement no. 643071.

References

[1] Baumann, I.; Westermann, P. (2016) Microbial production of short chain fatty acids from lignocellulosic biomass: current processes and market, Biomed Res. Int. ID 8469357.

[2] Jones R.J.; Massanet-Nicolau, J.; Mulder, M.J.J.; Premier, G.; Dinsdale, R.; Guwy, A.; (2017) Increased biohydrogen yields, volatile fatty acid production and substrate utilisation rates via the electrodialysis of a continually fed sucrose fermenter, Bioresour. Technol., 229: 46–52.

[3] Jones, R.J.; Massanet-Nicolau, J.; Guwy, A.; Premier, G.C.; Dinsdale, R.M.; Reilly, M. (2015) Removal and recovery of inhibitory volatile fatty acids from mixed acid fermentations by conventional electrodialysis, Bioresour. Technol., 189: 279–284.

[4] Longo, S.; Katsou, E.; Malamis, S.; Frison, N.; Renzi, D.; Fatone, F. (2014) Recovery of volatile fatty acids from fermentation of sewage sludge in municipal wastewater treatment plants, Bioresour. Technol., 175: 436–444.

[5] Choudhari, S.K.; Cerrone, F.; Woods, T.; Joyce, K.; O'Flaherty, V.; O'Connor, K.; Babu, R. (2015) Pervaporation separation of butyric acid from aqueous and anaerobic digestion (AD) solutions using PEBA based composite membranes, J. Ind. Eng. Chem., 23: 163–170.

[6] Zhou, M.; Yan, B.; Wong, J.W.C.; Zhang, Y. (2017) Enhanced volatile fatty acids production from anaerobic fermentation of food waste: A mini-review focusing on acidogenic metabolic pathways, Bioresour. Technol., 248: 68–78.

[7] Eregowda, T.; Matanhike, L.; Rene, E.R.; Lens, P.N.L. (2018) Performance of a biotrickling filter for anaerobic utilization of gas-phase methanol coupled to thiosulphate reduction and resource recovery through volatile fatty acids production, Bioresour. Technol., 263: 591–600.

[8] Martinez, G.A.; Rebecchi, S.; Decorti, D.; Domingos, J.M.B.; Natolino, A.; Del Rio, D.; Bertin, L.; Da Porto, C.; Fava, F. (2015) Towards multi-purpose biorefinery platforms for the valorisation of red grape pomace: production of polyphenols, volatile fatty acids, polyhydroxyalkanoates and biogas, Green Chem., 261–270.

[9] Anasthas, H.M.; Gaikar, V.G. (2001) Adsorption of acetic acid on ion-exchange resins in non-aqueous conditions, React. Funct. Polymers., 47: 23–35.

[10] Reyhanitash, E.; Zaalberg, B.; Kersten, S.R.A.; Schuur, B. (2016) Extraction of volatile fatty acids from fermented wastewater, Sep. Purif. Technol., 161: 61–68.

[11] Tugtas, A.E. (2011) Fermentative organic acid production and separation, Fen Bilim. Derg., 23: 70–78.

[12] Djas, M.; Henczka, M. (2018) Reactive extraction of carboxylic acids using organic solvents and supercritical fluids: A review, Sep. Purif. Technol., 201: 106–119.

[13] Pan, X.R.; Li, W.W.; Huang, L.; Liu, H.Q.; Wang, Y.K.; Geng, Y.K.; Kwan-Sing Lam, P.; Yu, H.Q. (2018) Recovery of high-concentration volatile fatty acids from wastewater using an acidogenesis-electrodialysis integrated system, Bioresour. Technol., 260: 61–67.

[14] Rebecchi, S.; Pinelli, D.; Bertin, L.; Zama, F.; Fava, F.; Frascari, D. (2016) Volatile fatty acids recovery from the effluent of an acidogenic digestion process fed with grape pomace by adsorption on ion exchange resins, Chem. Eng. J., 306: 629–639.

[15] Zhang, Y.; Angelidaki, I. (2015) Bioelectrochemical recovery of waste-derived volatile fatty acids and production of hydrogen and alkali, Water Res., 81: 188–195.

[16] Wu, W.L.; Zhou, Q.; Yuan, L.; Deng, X.L.; Long, S.R.; Huang, C.L,; Cui, H.P.; Huo, L.S.; Zheng, J.X. (2016) Equilibrium, kinetic, and thermodynamic Studies for crude structured-lipid deacidification using strong-base anion exchange resin, J. Chem. Eng. Data., 61: 1876–1885.

[17] López-garzón, C.S.; Straathof, A.J.J. (2014) Recovery of carboxylic acids produced by fermentation, Biotechnol. Adv., 32: 873–904.

[18] Da Silva, A.H.; Miranda, E.A. (2013) Adsorption/desorption of organic acids onto different adsorbents for their recovery from fermentation broths, J. Chem. Eng. Data., 58: 1454–1463.

[19] Yousuf, A.; Bonk, F.; Bastidas-Oyanedel, J.R.; Schmidt, J.E. (2016) Recovery of carboxylic acids produced during dark fermentation of food waste by adsorption on Amberlite IRA-67 and activated carbon, Bioresour. Technol., 217: 137–140.

[20] Reyhanitash, E.; Kersten, S.R.A.; Schuur, B. (2017) Recovery of volatile fatty acids from fermented wastewater by adsorption, ACS Sustain. Chem. Eng., 5: 9176–9184.

[21] Pradhan, N.; Rene, E.R.; Lens, P.N.L.; Dipasquale, L.; D'Ippolito, G.; Fontana, A.; Panico, A.; Esposito, G. (2017) Adsorption behaviour of lactic acid on granular activated carbon and anionic resins: Thermodynamics, isotherms and kinetic studies, Energies., 10: 1–16.

[22] Uslu, H.; Bayazit, S. (2010) Adsorption equilibrium data for acetic acid and glycolic acid onto amberlite, J. Chem. Eng. Data., 298: 1295–1299.

[23] Tan, L.C.; Calix, E.M.; Rene, E.R.; Nancharaiah, Y.V.; van Hullebusch, E.D.; Lens, P.N.L. (2018) Amberlite IRA-900 ion exchange resin for the sorption of selenate and sulfate: Equilibrium, Kinetic, and regeneration studies, J. Environ. Eng., 144:

[24] Sheha, R.R.; El-Shazly, E.A. (2010) Kinetics and equilibrium modeling of Se(IV) removal from aqueous solutions using metal oxides, Chem. Eng. J., 160: 63–71.

[25] Ahmaruzzaman, M. (2008) Adsorption of phenolic compounds on low-cost adsorbents: A review, Adv. Colloid Interface Sci., 143: 48–67.

[26] Sun, W.; Pan, W.; Wang, F.; Xu, N. (2015) Removal of Se(IV) and Se(VI) by MFe2O4 nanoparticles from aqueous solution, Chem. Eng. J., 273: 353–362.

[27] Guerra, D.J.L.; Mello, I.; Freitas, L.R.; Resende, R.; Silva, R.A.R. (2014) Equilibrium, thermodynamic, and kinetic of Cr(VI) adsorption using a modified and unmodified bentonite clay, Int. J. Min. Sci. Technol., 24: 525–535.

[28] Cao, X.; Yun, H.S.; Koo, Y.M. (2002) Recovery of L-(+)-lactic acid by anion exchange resin Amberlite IRA-400, Biochem. Eng. J., 11: 189–196.

[29] Foo, K.Y.; Hameed, B.H.; (2010) Insights into the modeling of adsorption isotherm systems. Chem. Eng. J., 156: 2-10.

[30] Bansal, R.C.; Goyal, M. (2005) Activated Carbon Adsorption, CRC Press, Boca Raton, USA, pp: 520.

[31] Baig, K.S.; Doan, H.D.; Wu, J. (2009) Multicomponent isotherms for biosorption of Ni^{2+} and Zn^{2+}, Desalination., 249: 429–439.

[32] Ebadi, A.; Soltan Mohammadzadeh, J.S.; Khudiev, A. (2009) What is the correct form of BET isotherm for modelling liquid phase adsorption?, Adsorption., 15: 65–73.

[33] Bayazit, Ş.S.; Inci, I.; Uslu, H. (2011) Adsorption of lactic acid from model fermentation broth onto activated carbon and amberlite IRA-67, J. Chem. Eng. Data., 56: 1751–1754.

[34] Kinnunen, V.; Ylä-Outinen, A.; Rintala, J. (2015) Mesophilic anaerobic digestion of pulp and paper industry biosludge–long-term reactor performance and effects of thermal pretreatment, Water Res., 87: 105-111.

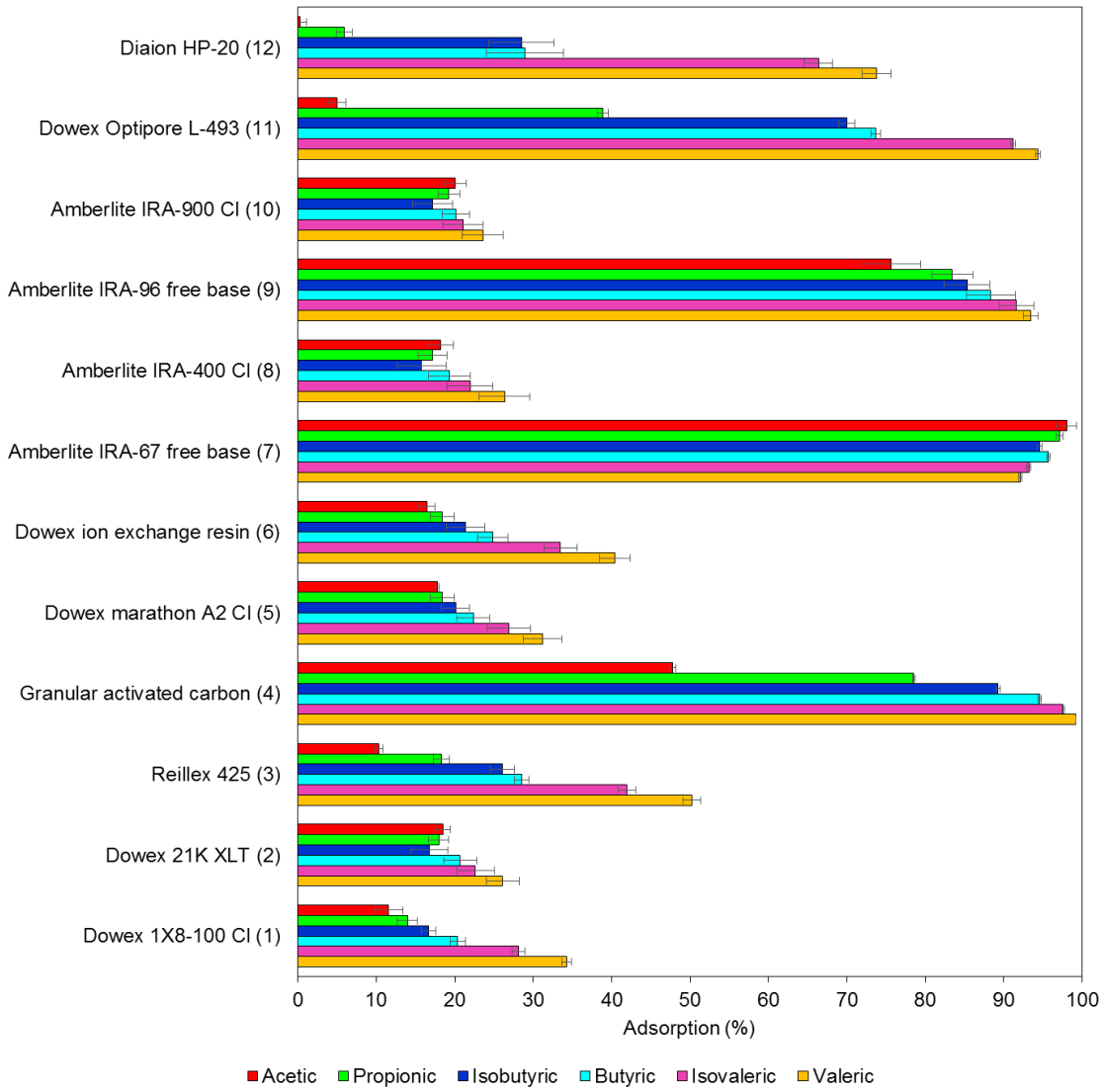

Figure 1. Screening of various commercial resins and GAC for VFA adsorption.

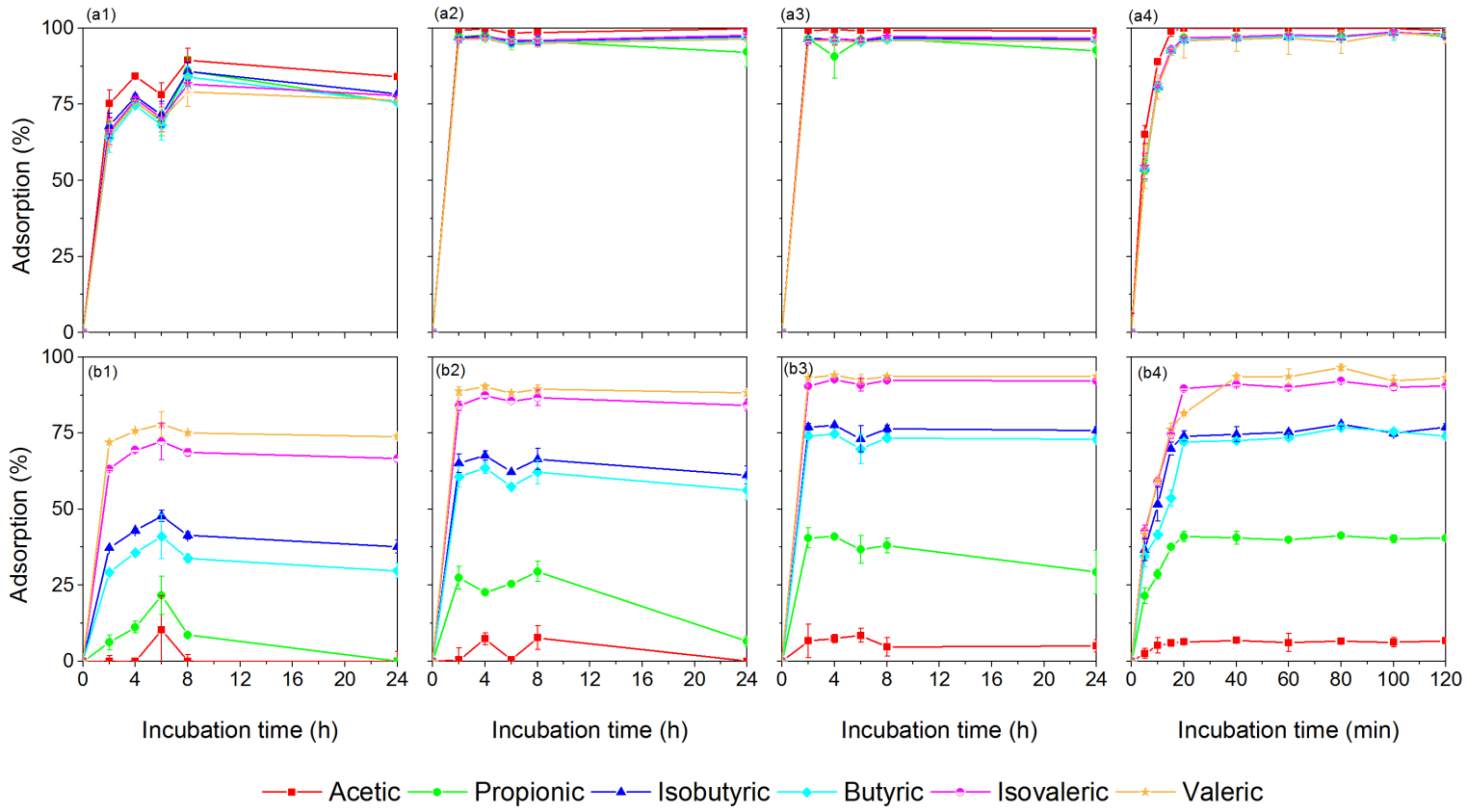

Figure 2: Effect of contact time on the adsorption of VFA by different resins: (a) Amberlite and (b) Dowex at resin concentrations of (1) 25, (2) 50, (3) 75 g/L, respectively. (a4) and (b4) are the profiles of VFA adsorption (%) for Amberlite and Dowex, respectively, at an incubation time of 120 min.

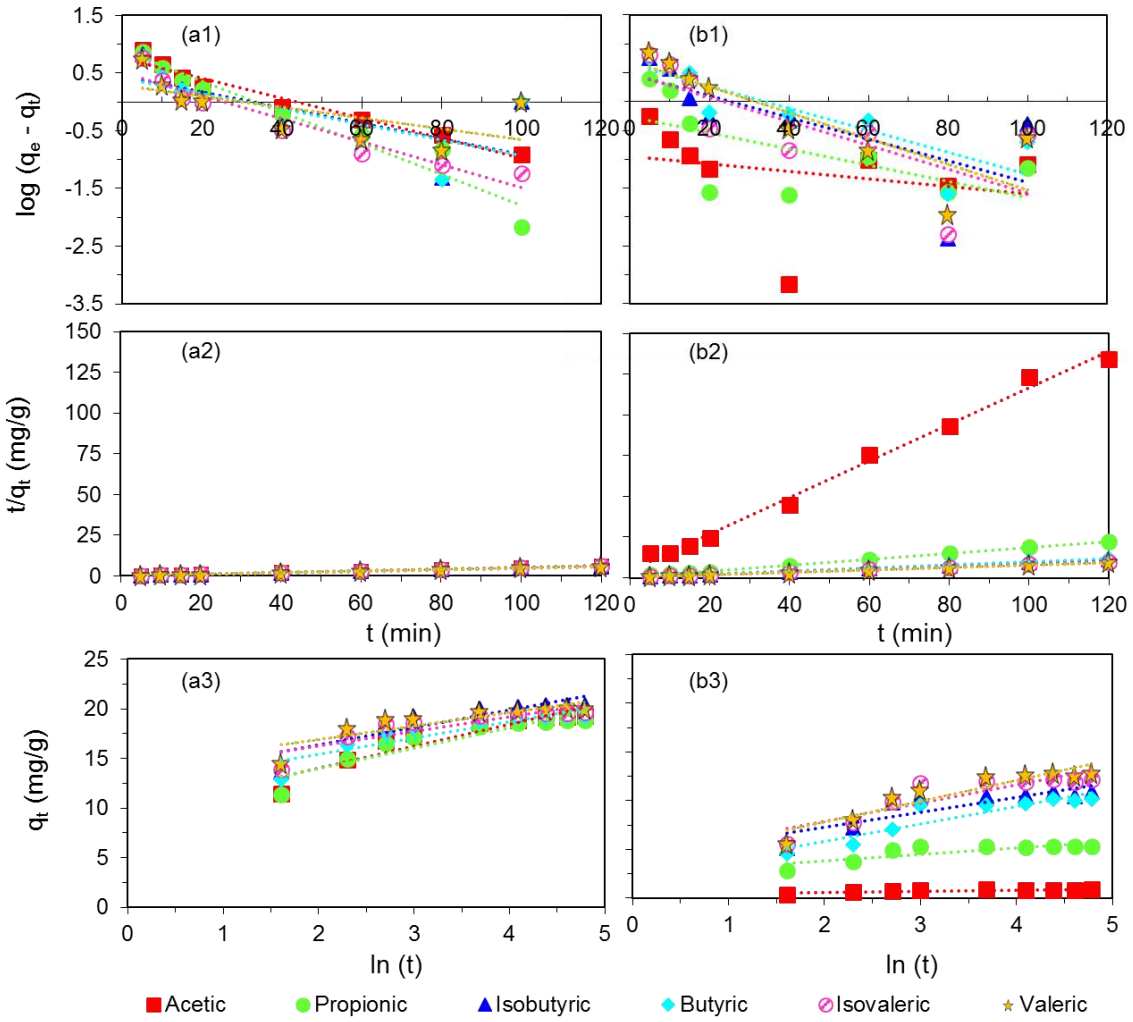

Figure 3: VFA adsorption kinetics data for: (a) Amberlite and (b) Dowex, respectively, fitted to: (1) pseudo-first order, (2) pseudo-second order, and (3) Elovich kinetic model at an initial concentration of 6 g/L of total VFA (1 g/L each) and a resin concentration of 50 g/L of Amberlite and 75 g/L of Dowex. Data points represent the experimental data, while the dotted lines are the model fits.

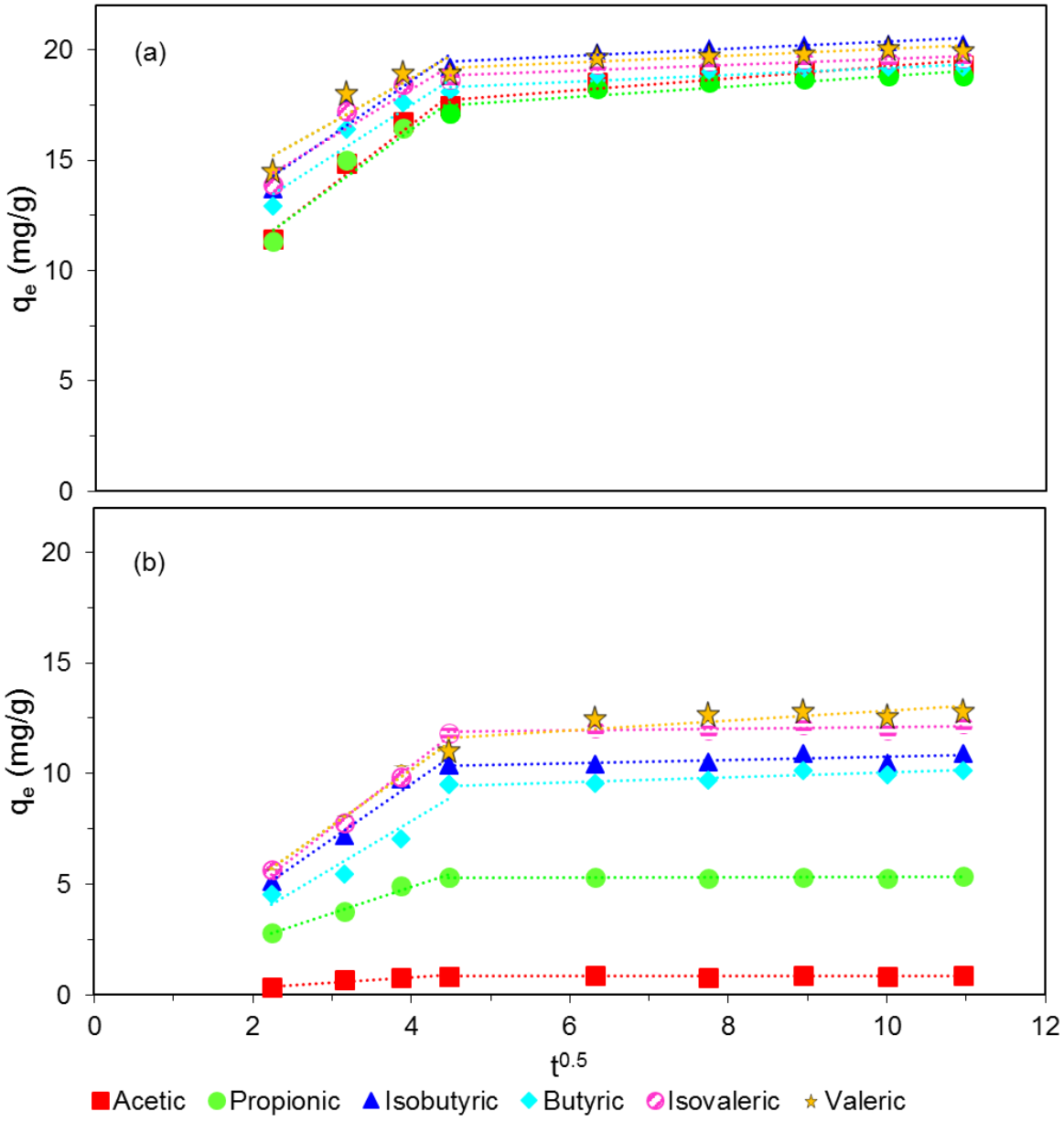

Figure 4: Experimental data fitted to the intraparticle diffusion model for VFA adsorption by: (a) Amberlite and (b) Dowex.

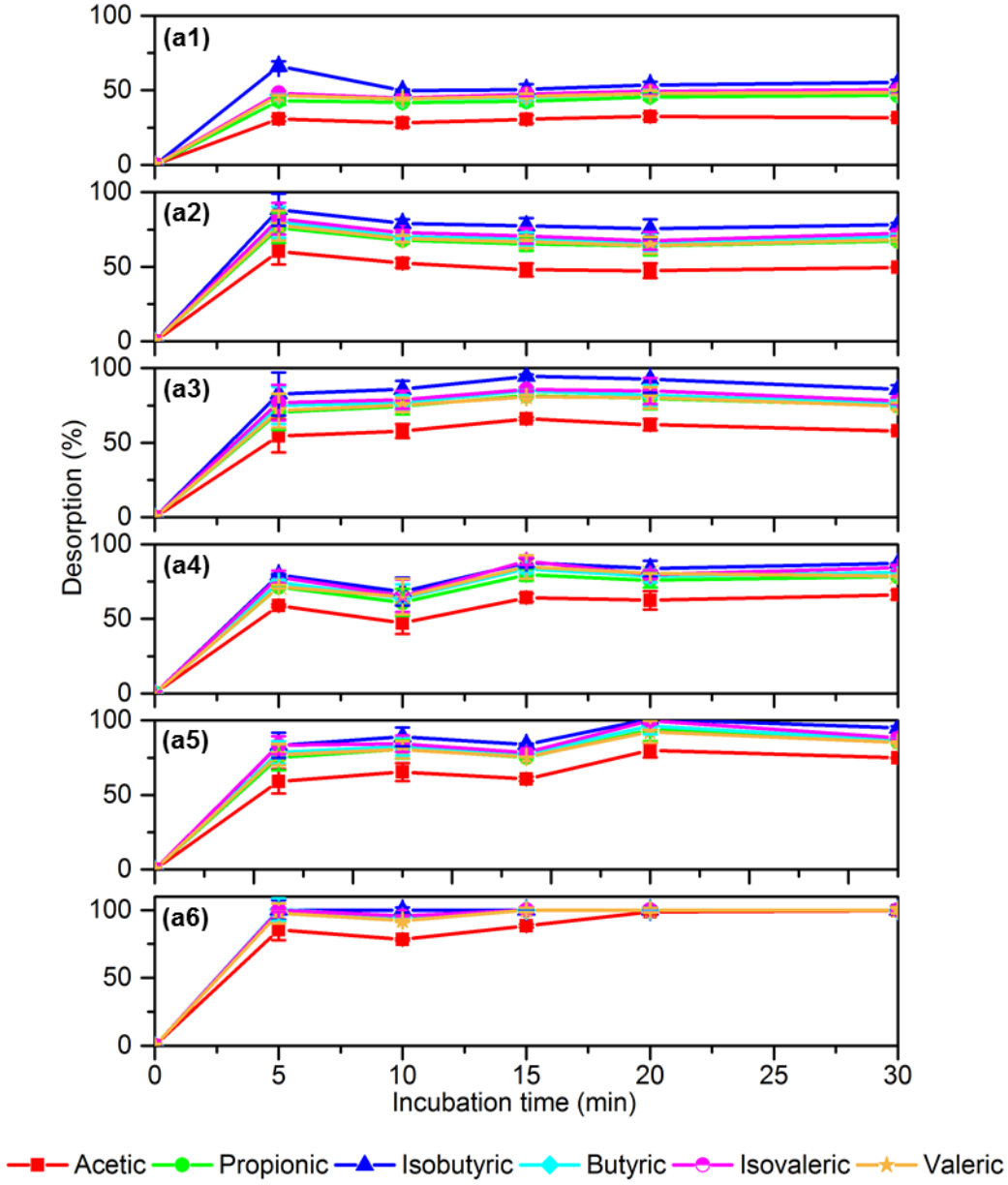

Figure 5: Desorption of VFA from Amberlite using: (a) 45, (b) 60, (c) 70, (d) 75, (e) 80, and (f) 100 mM NaOH.

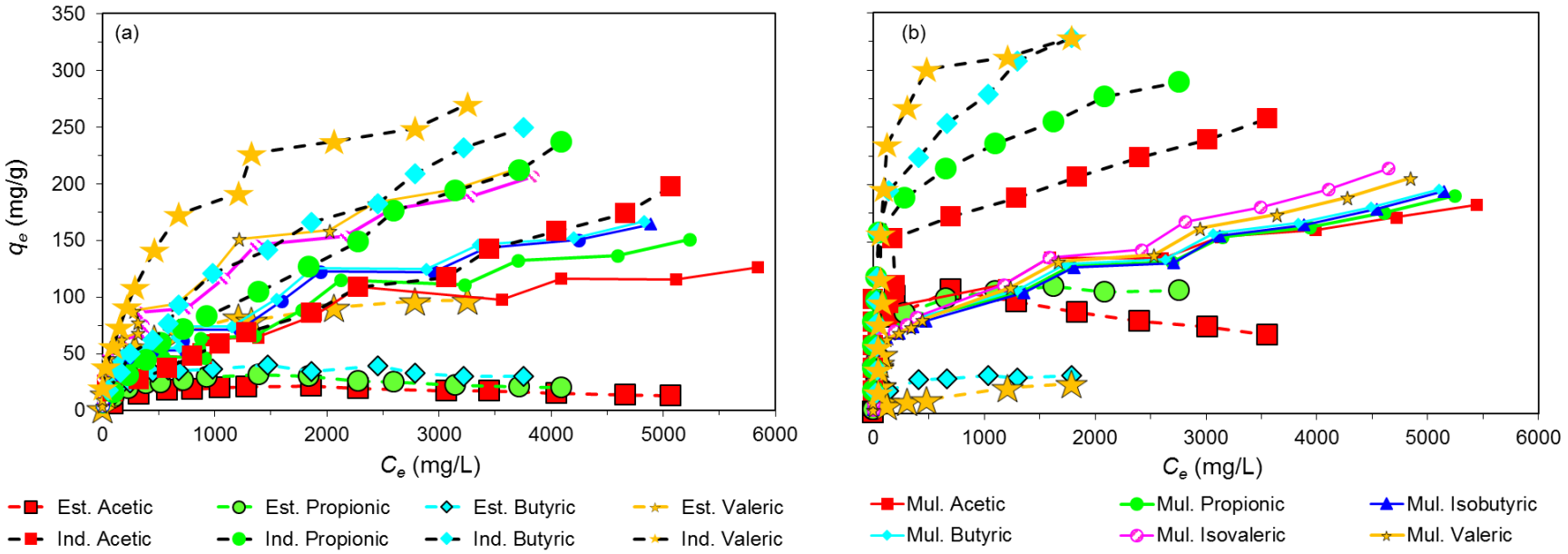

Figure 6: Adsorption capacity (q_e) vs equilibrium concentration (C_e) plot for: (a) Amberlite and (b) Dowex. Comparison between q_e in single component batch system is denoted with prefix 'Ind.', estimated q_e for a multi-component system is denoted with the prefix 'Est.', and the experiment based q_e in a real multi-component batch system is denoted with the prefix 'Mul.'

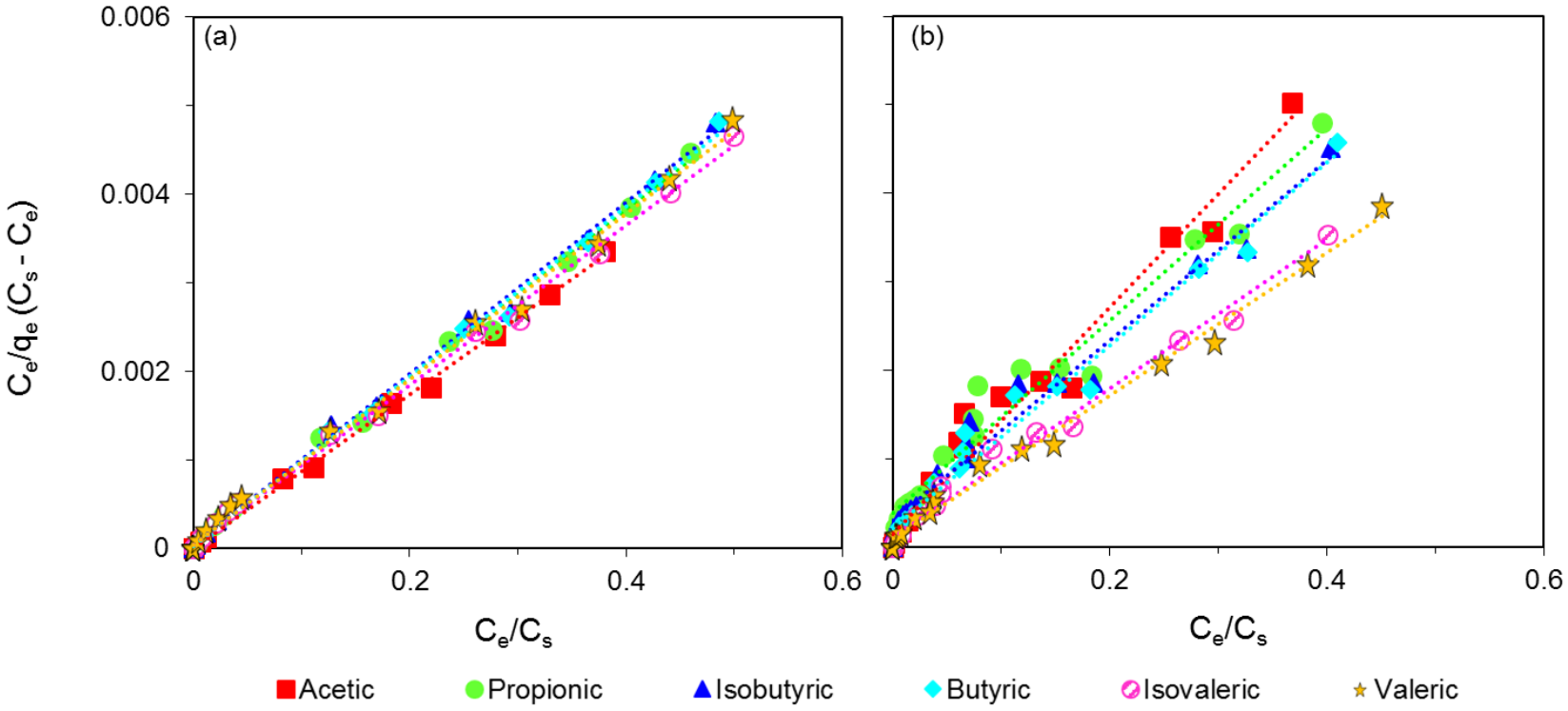

Figure 7: Equilibrium adsorption isotherm data fitted to the BET multi-component model for: (a) Amberlite and (b) Dowex.

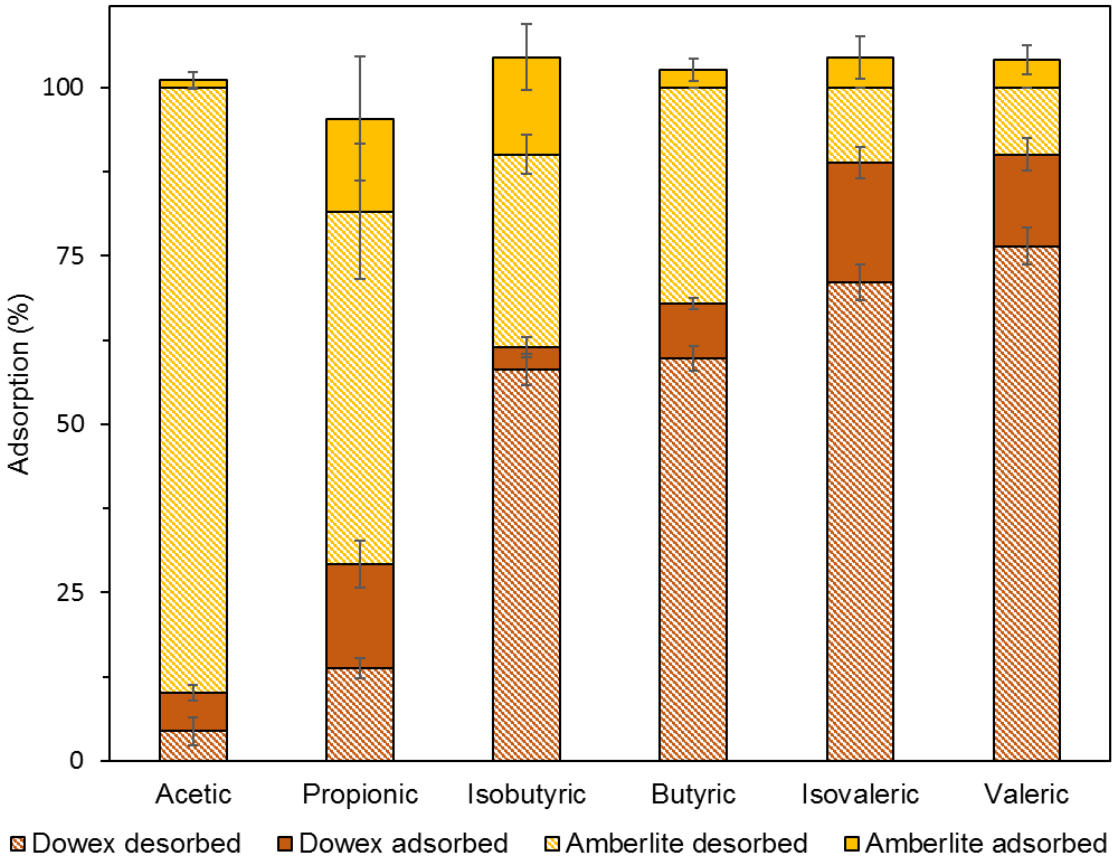

Figure 8: Separation of acetic acid due to selective adsorption of VFA on Amberlite and Dowex.

6 Table 1: Different aspects of VFA adsorption reported in different studies.

Adsorption medium	Adsorbed compound	Adsorption resin	Key objective	Reference
Water	Acetic acid and glycolic acid	Amberlite IRA-67	Thermodynamic parameters and the effect of temperature	Uslu and Bayazit (2010)
A non-aqueous mixture of ethyl acetate and ethanol	Acetic acid	Indion 850, Tuision A-8X MP, Indion 810	Adsorption equilibrium	Anasthas and Gaikar (2001)
Artificial dark fermentation effluent containing chlorides, sulphates and phosphates and	Acetic, propionic, butyric and lactic acid	Lewatit VP OC 1065, Amberlite IRA96 RF, Amberlite IRA96 SB, and Lewatit VP OC 1064 MD PH	Adsorption from a complex solution mimicking fermented wastewater and desorption through nitrogen stripping at different temperatures for resin regeneration	Reyhanitash et al. (2017)
Binary systems using water, ethanol and n-propanol as solvents	Acetic, propionic and butyric acid	Purolite A133S and activated carbon	Adsorption and desorption using a multi-stage counter-current process	Da Silva and Miranda (2013)
Dark fermentation broth	Lactic, acetic and butyric acid	Amberlite IRA-67 and activated carbon	Adsorption and the effect of pH	Yousuf et al. (2016)
Acidogenic digestion effluent	Acetic, propionic, isobutyric, butyric, isovaleric, valeric, and caproic acid	Sepra NH2, Amberlyst A21, Sepra SAX, Sepra ZT-SAX	Adsorption and desorption using a basified ethanol and predicting the ion exchange capacity of the resin using an ion exchange model	Rebecchi et al. (2016)
Water	Acetic, propionic, isobutyric, butyric, isovaleric acid valeric acid	Amberlite IRA-67 and Dowex optipore L-493	Isotherm and kinetics of VFA adsorption and selective recovery using Amberlite IRA-67 and Dowex optipore L-493 in sequential batch mode	This study

7

Table 2: List of anion-exchange resins screened for VFA adsorption

Resin number	Adsorbate	Manufacturer	Matrix and active site	Type	Active group
R1	Dowex 1X8-100 (Cl)	Sigma-Aldrich	styrene-divinylbenzene	type 1, strongly basic	trimethylbenzyl ammonium,
R2	Dowex 21K XLT	Supelco	styrene-divinylbenzene	type 1, strongly basic	trimethylbenzyl ammonium
R3	Reillex 425	Aldrich	Poly(4-inylpyridine), 25% cross-linked with divinylbenzene		pyridine
R4	Granular activated carbon (GAC)				
R5	Dowex marathon A2 (Cl)	Sigma-Aldrich	styrene-divinylbenzene	type 2, weakly basic	dimethyl-2-hydroxyethylbenzyl ammonium,
R6	Dowex ion exchange resin		standard anion exchange resin		
R7	Amberlite IRA-67 free base	Aldrich	styrene-divinylbenzene	type 2, weakly basic	polyamine,
R8	Amberlite IRA-400 (Cl)	Aldrich	styrene-divinylbenzene	type 1, strongly basic	trialkylbenzyl ammonium,
R9	Amberlite IRA-96 free base	Sigma-Aldrich	styrene-divinylbenzene	type 2, weakly basic	polyamine,
R10	Amberlite IRA-900 (Cl)	Sigma-Aldrich	styrene-divinylbenzene copolymer	type 1 strongly basic	trialkylbenzyl ammonium,
R11	Dowex Optipore L-493	Sigma-Aldrich	polystyrene- divinylbenzene (PS-DVB)		none
R12	Diaion HP-20	Supelco	styrene-divinylbenzene		none

11 Table 3: Physical properties of the resins selected for the VFA adsorption studies

Ion exchange resin	**Amberlite® IRA-67 free base**	**Dowex Optipore® L-493**
Particle size [mm]	0.50-0.75	0.2-0.3
BET surface area [m^2/g]	8.4	1048
Pore volume [mL/g]	0.007	0.72-0.79
Average pore diameter [nm]	3.3-3.35	2.75-3.0
Bulk density [g/L]	700	680
Total exchange capacity [eq/L]	≥ 1.60	0.6

12

13

14

Table 4: List of differential and linear form of adsorption kinetic and isotherm model equations

	Differential form	Linear form	Plot	
Pseudo-first order kinetic model	$\frac{dq_t}{dt} = K_1(q_e - q_t)$	$\log(q_e - q_t) = \log q_e - (\frac{K_1}{2.303})t$	$\log(q_e - q_t)$ vs. t	(Eq. 3)
Elovich kinetic model	$\frac{dq_t}{dt} = \alpha e^{-\beta q_t}$	$q_t = \beta \ln \alpha\beta + \ln\ t$	q_t vs. $\ln t$	(Eq. 4)
Pseudo-second order kinetic model	$\frac{dq_t}{dt} = K_2(q_e - q_t)^2$	$\frac{t}{q_t} = \frac{1}{K_2 q_e^2} + \frac{1}{q_e}t = \frac{1}{h_0} + \frac{1}{q_e}t$	$\frac{t}{q_t}$ vs. t	(Eq. 5)
Intra-particle diffusion model		$q_t = K_{id}t^{0.5} + C_{id}$	q_t vs. $t^{0.5}$	(Eq. 6)
Langmuir single component isotherm model	$q_e = \frac{Q_o b C_e}{1 + bC_e}$	$\frac{C_e}{q_e} = \frac{1}{bQ_o} + \frac{C_e}{Q_o}$	$\frac{C_e}{q_e}$ vs. C_e	(Eq. 7)
Langmuir multi-component isotherm model		$q_{ei} = \frac{Q_{oi} b_i C_{ei}}{1 + \sum b_i C_{ei}}$		(Eq. 8)
BET (multilayer) isotherm model	$q_e = q_s \frac{K_S C_e}{(C_s - C_e)[1 + (K_S - 1)\frac{C_e}{C_s}]}$	$\frac{C_e}{q_e(C_s - C_e)} = \frac{1}{q_s K_S} + \frac{(K_S - 1)}{q_s K_S} \times \frac{C_e}{C_s}$	$\frac{C_e}{q_e(C_s - C_e)}$ vs. $\frac{C_e}{C_s}$	(Eq. 9)

Table 5: Pseudo-second order model parameters for Amberlite and Dowex

	Amberlite						**Dowex**					
Multi-component VFA	Acetic	Propionic	Isobutyric	Butyric	Isovaleric	Valeric	Acetic	Propionic	Isobutyric	Butyric	Isovaleric	Valeric
q_e [mg/g]	19.82	19.32	20.74	19.53	19.87	20.32	0.89	5.49	11.18	10.75	12.64	13.44
h_0 [mg/g.min]	6.38	6.96	11.33	10.67	13.43	14.14	0.23	2.03	3.01	1.66	3.07	2.65
K_2 [g/mg.min]	0.0163	0.0187	0.0263	0.0280	0.0340	0.0342	0.285	0.067	0.024	0.021	0.019	0.015
R^2	0.999	0.999	0.999	0.999	0.999	0.999	0.995	0.998	0.998	0.996	0.998	0.998

Note: Experiments were performed at room temperature (22 ± 2 ºC) with 1 g/L each of the VFA

24 Table 6: Intra-particle diffusion model parameters to describe the mechanism of VFA adsorption by Amberlite and Dowex

25

26

	Amberlite						**Dowex**					
	Acetic	Propionic	Isobutyric	Butyric	Isovaleric	Valeric	Acetic	Propionic	Isobutyric	Butyric	Isovaleric	Valeric
K_{id} [mg/g.min$^{-0.5}$]	2.74	2.62	2.46	2.32	2.15	2.01	0.22	1.18	2.48	2.15	2.77	2.52
C_{id} [g/mg]	5.70	5.97	8.80	8.29	9.66	10.73	0.20	1.95	3.08	1.85	2.97	2.89
R^2	0.99	0.973	0.959	0.938	0.95	0.962	0.912	0.981	0.72	0.91	0.99	0.98

27 Table 7: Langmuir single-component and multi-component, and BET isotherm model parameters for Amberlite and Dowex

	Langmuir model for single-component system											
	Single component system						Estimated values for multi component system					
	Amberlite			Dowex			Amberlite			Dowex		
	q_m [mg/g]	$B \times 10^{-3}$ [L/mg]	R^2 -	q_m [mg/g]	$B \times 10^{-3}$ [L/mg]	R^2 -	q_m [mg/g]	$B \times 10^{-2}$ [L/mg]	R^2 -	q_m [mg/g]	$B \times 10^{-3}$ [L/mg]	R^2 -
Acetic acid	246	7.52	0.983	218	0.4	0.99	75	3.05	0.991	13.4	3.3	0.979
Propionic acid	282	6.31	0.991	227	0.52	0.99	110.2	2.01	1.000	21.0	5.8	0.985
Isobutyric acid	-	-	-	-	-	-	-	-	-	-	-	-
Butyric acid	336	7.17	0.985	247	0.98	0.97	33.1	4.34	0.999	31.7	21.4	0.988
Isovaleric acid	-	-	-	-	-	-	-	-	-	-	-	-
Valeric acid	360	6.24	0.975	263	2.76	0.98	25.2	1.02	0.946	102.3	4.24	0.998

	Multi-component system												
	Langmuir model						BET model						
	Amberlite			Dowex			Amberlite				Dowex			
	q_m [mg/g]	$B \times 10^{-3}$ [L/mg]	R^2 -	q_m [mg/g]	$B \times 10^{-3}$ [L/mg]	R^2 -	q_s [mg/g]	$K_S \times 10^{-3}$ [L/mg]	$K_L \times 10^{-5}$ [L/mg]	R^2	q_s [mg/g]	$K_S \times 10^{-3}$ [L/mg]	$K_L \times 10^{-5}$ [L/mg]	R^2
Acetic acid	169.4	9.38	0.983	124.1	0.99	0.933	115.3	38.11	7.00	0.999	76.0	1.75	7.2	0.983
Propionic acid	175.4	4.36	0.966	161.0	0.91	0.890	106.2	12.2	8.77	0.997	87.6	1.70	8.62	0.980
Isobutyric acid	178.1	3.91	0.958	172.1	1.24	0.915	104.1	10.9	9.40	0.997	93.4	2.73	9.52	0.985
Butyric acid	179.6	4.52	0.963	168.2	1.62	0.921	104.8	14.38	9.52	0.997	92.9	3.92	9.75	0.986
Isovaleric acid	195.3	4.27	0.955	199.0	3.19	0.939	111.3	12.68	10.8	0.997	114.5	8.58	12.2	0.991
Valeric acid	189.4	3.77	0.956	209.1	3.08	0.951	107.6	10.61	10.3	0.997	122.3	7.74	12.27	0.992

28